In Situ Photo-Cross-Linking of Cinnamate Functionalized Poly(methyl methacrylate-*co*-2-hydroxyethyl acrylate) Fibers during Electrospinning

Pankaj Gupta,[†] Scott R. Trenor,[‡] Timothy E. Long,[‡] and Garth L. Wilkes*,[†]

Departments of Chemical Engineering & Chemistry, Polymer Materials & Interfaces Laboratory, Virginia Polytechnic Institute & State University, Blacksburg, Virginia 24061

Received June 11, 2004; Revised Manuscript Received August 26, 2004

ABSTRACT: A novel methodology for in situ cross-linking of polymeric fibers during electrospinning is described. The electrospinning apparatus was modified to facilitate UV irradiation of the electrospun fibers while in flight to the collector target. Three polymers with different mol % of the photoreactive cinnamate functional group (4, 9, and 13 mol %) were synthesized and utilized for this study. Fibers of cinnamate functionalized poly(methyl methacrylate-*co*-2-hydroxyethyl acrylate) were cross-linked in situ by UV irradiation during electrospinning. Subsequent FTIR measurements on irradiated and non-irradiated electrospun fibers indicated both [$2\pi + 2\pi$] cycloaddition of the vinylene C=C and trans−cis photoisomerization of the cinnamate group. Furthermore, the irradiated copolymers were observed to form insoluble gels which indicated that the photodimerization was the primary photoprocess during UV irradiation, leading to the formation of a cross-linked network. As expected, it was found that the gel fraction increased with increasing mol % of the cinnamate species.

1. Introduction

Polymers that are sensitive to ultraviolet (UV) irradiation have been widely utilized as photoresists. For instance, in the manufacture of printed circuit boards,[1] negative photoresists are coated on a conducting substrate. A patterned mask placed over the coated substrate then imprints a conducting circuit when the substrate is washed with a solvent to remove the non-irradiated photoresist. Conventional negative-working photoresists based on poly(vinyl cinnamate) (PVCi) and its derivatives have played a leading role in the scientific development of photopolymers since their invention more than four decades ago.[2] The photofunctionality of PVCi arises from photodimerization that leads to insolubilization due to the formation of cross-links. In the late 1970s, it was reported[3,4] that the photoinduced chemical transformation of PVCi and its derivatives resulted in a novel optical property, i.e., induction of birefringence in thin films of PVCi upon exposure to linearly polarized photoirradiation. The further advancement in polarization photochemistry of ultrathin films leading to regulation of the orientation of liquid crystal (LC) molecules[5−11] resulted in an enhanced interest in PVCi. More specifically, it has been observed that PVCi and its derivatives induce the alignment of LCs in contact with the film surface upon irradiation with linearly polarized ultraviolet light. In addition to these unique properties, the ability of the cinnamate group to undergo rapid photodimerization without the addition of a photoinitiator is critically important in the context of the present investigation, as will become more apparent later.

The photochemistry of cinnamates involves two photoreactions upon irradiation in the ultraviolet-B (UVB) region of the electromagnetic spectrum:[12−14] the trans−cis isomerization that is favored in the early stages of UV irradiation[15−17] (Scheme 1) and the photodimerization from head-to-head and head-to-tail [$2\pi + 2\pi$] cycloaddition, leading to the formation of a cyclobutane ring (Scheme 2). It is believed that during UV irradiation, photodimerization is the major photoprocess, while the trans−cis photoisomerization is the minor photoprocess.[18,19] In the present study, cinnamate functionalized polymers were electrospun and *simultaneously* irradiated in the UVB region to produce cross-linked fibers.

Scheme 1. Trans−Cis Photoisomerization of the Cinnamoyl Moiety

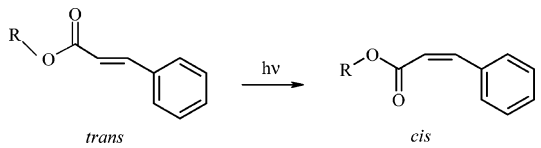

Scheme 2. (a) Head-to-Head and (b) Head-to-Tail Photodimerization of the Cinnamoyl Moiety

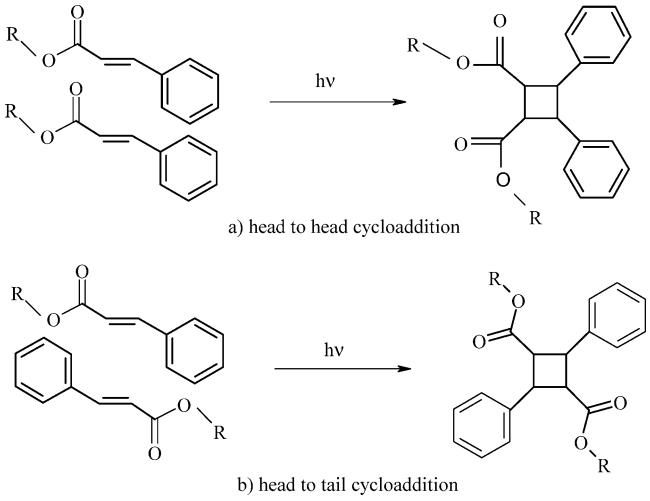

Electrospinning is a unique process to produce submicron polymeric fibers in the average diameter range of 100 nm−5 μm.[20−23] Fibers produced by this approach

[†] Department of Chemical Engineering.
[‡] Department of Chemistry.
* Corresponding author: e-mail gwilkes@vt.edu, Tel (540) 231-5498.

10.1021/ma048844g CCC: $27.50
Published on Web 10/26/2004

have a diameter that is at least 1 or 2 orders of magnitude smaller than those produced by conventional fiber production methods like melt or solution spinning.[24] In a typical electrospinning process, a jet is ejected from the surface of a charged polymer solution when the applied electric field strength (and consequently the electrostatic repulsion on the surface of the fluid) overcomes the surface tension. At a critical point, defined as the equilibrium between the electrostatic repulsion and the surface tension of the fluid, the free surface of the fluid takes a conical shape, also commonly referred to as the Taylor cone.[25] A jet that is ejected from the surface of this Taylor cone rapidly travels to the collector target located at some distance from the charged polymer solution under the influence of the electric field. Solidified polymer filaments are collected on the target as the jet dries. It is well established that the jet undergoes a series of electrically driven bending instabilities[26−28] that gives rise to a series of looping and spiraling motions beginning in a region close to ejection of the jet. As the jet travels to the target, it elongates to minimize the instability caused by the repulsive electrostatic charges, thereby causing the jet to undergo large amounts of plastic stretching that consequently leads to a significant reduction in its diameter. Recent efforts in our laboratories have developed predictive models that correlate solution rheology to fiber diameter.[29] These extremely small diameter electrospun fibers possess a high aspect ratio that lead to a larger specific surface. As a result, they have potential applications ranging from optical[30] and chemosensor materials,[31] nanocomposite materials,[32] nanofibers with specific surface chemistry[33] to tissue scaffolds, wound dressings, drug delivery systems,[34−36] filtration, and protective clothing.[37]

Recently, researchers have also employed several post-electrospinning processing techniques to produce electrospun fibers that find utility in novel applications. For instance, electrospun fibers of 2-acrylamido-2-methyl-1-propanesulfonic acid-doped polyaniline were coated uniformly with thin films of nickel by an electroless deposition technique.[38] The resulting high surface area metal-coated fibrous polymer substrates displayed high conductivity, thereby combining the dual benefits of electrospinning (to produce high surface area fibers) with electroless metal deposition (to make conducting polymer substrates). In a different study, ultrafine mats of oxidized cellulose were prepared by electrospinning of cellulose acetate followed by its subsequent deacetylation and oxidation. Direct electrospinning of oxidized cellulose is not feasible because of its low solubility in most organic solvents. As a result, post-deacetylation and oxidation of electrospun cellulose acetate were performed to produce mats that potentially serve as flexible adhesion barriers and as immobilizing matrices for various drugs, enzymes, and proteins.[39] Another post-electrospinning process that more specifically relates to the present study involved cross-linking of photocurable poly(vinyl alcohol) (PVA) fibers. Electrospun mats of partially esterified PVA containing thienyl acrylate groups were subjected to UV irradiation ($\lambda > 300$ nm) to produce cross-linked PVA fibers. The UV-irradiated fibers displayed excellent water stability, in stark contrast to the PVA fibers produced without UV irradiation.[40]

In the experimental approaches that are discussed above, the post-electrospinning processes involved metal-coating, oxidation, or cross-linking of the electrospun substrate, which enhanced the fiber properties and lead to new applications. In the following sections, we will discuss a new method that involves *simultaneous* cross-linking and electrospinning of photo-cross-linkable polymers. A new device that was designed and fabricated especially to facilitate these two processes to occur in tandem will be described in detail. Using this novel technique, post-electrospinning operations are eliminated, resulting in a more time-efficient and dynamic process. It should be noted that, in addition to the design of the device, the choice of the photocurable functional group is also very important. As mentioned earlier, the cinnamate group undergoes a rapid photodimerization in the UVB region without the addition of any photoinitiators.

In the present study, poly(methyl methacrylate-*co*-hydroxyethyl acrylate) [poly(MMA-*co*-HEA)] was synthesized and subsequently functionalized with cinnamoyl chloride via a quantitative esterification reaction. The cinnamate functionalized polymers were then irradiated with UV in situ during the electrospinning process to form cross-linked fibers in a single processing step. The extent of the photoreactions was monitored with Fourier transform infrared (FTIR) spectroscopy and gel fraction analysis. The morphology of the electrospun mat before and after UV irradiation was investigated using scanning electron microscopy (SEM).

2. Experimental Section

2.1. Materials. Cinnamoyl chloride, ethyl acetate, and 2,2′-azobis(isobutyronitrile) (AIBN) and dimethylformamide (DMF) were purchased from Sigma Aldrich. Methyl methacrylate (MMA) and 2-hydroxyethyl acrylate (HEA), also purchased from Sigma Aldrich, were passed through a neutral alumina column to remove radical inhibitors. Tetrahydrofuran (THF) was distilled from sodium/benzophenone under a nitrogen atmosphere prior to polymer/acid chloride reactions.

2.2. Synthesis and Characterization of 85:15 mol % MMA:HEA Precursor Copolymers. MMA (40.0 g, 465 mmol) and HEA (9.52 g, 81.9 mmol) were added to a 500 mL round-bottomed flask containing a magnetic stir bar. This reaction mixture was diluted with ethyl acetate (205 mL, 80 vol %) followed by the addition of the initiator, AIBN (40.3 mg, 0.1 wt %), to the reaction vessel equipped with a water condenser. The reaction mixture was purged with nitrogen gas for 10 min and maintained at 75 °C. Polymerization was allowed to occur for 24 h. The resultant copolymer was precipitated into methanol followed by drying in a vacuum at 65 °C for 24 h. ^{1}H NMR spectroscopy and gel permeation chromatography (GPC) was used to determine the molecular weight and content of HEA incorporated in the copolymer.

^{1}H NMR spectra were recorded using a Varian Unity 400 MHz spectrometer at 25 °C in $CDCl_3$. Absolute number- and weight-average molecular weights of the precursor copolymers were determined at 40 °C in THF (HPLC grade) at 1 mL/min on a Waters 707 Autosampler GPC equipped with three in-line PLgel 5 mm Mixed-C columns and an in-line Wyatt Technology Corp. miniDAWN multiple angle laser light scattering (MALLS) detector.

2.3. Functionalization of Poly(MMA-*co*-HEA) with Cinnamoyl Chloride and Its Characterization. Poly(MMA-*co*-HEA) (5.00 g) was dissolved in 40 mL of freshly distilled THF. Triethylamine (0.644 g, 6.37 mmol) was added to the reaction mixture followed by stirring under a nitrogen purge. Cinnamoyl chloride (1.06 g, 6.37 mmol) was dissolved in 5 mL of distilled THF and added drop-by-drop via an addition funnel to the reaction mixture. This reaction mixture was stirred overnight at 0 °C and stored under a nitrogen blanket with the reaction vessel covered in aluminum foil to avoid any ambient photoreactions that might be induced by

Scheme 3. Functionalization of Poly(MMA-*co*-HEA) with Cinnamoyl Chloride

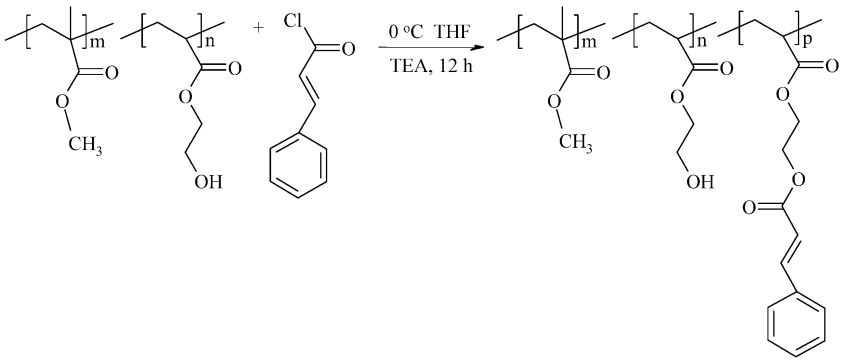

Table 1. Chemical Composition of the Functionalized Copolymers and Zero Shear Rate Viscosity (η_0) of Their Respective 20 wt % Solutions in DMF

sample	mol % MMA (x)	mol % HEA (y)	mol % cinnamate (z)	T_g (°C)	η_0 of a 20 wt % solution in DMF (Pa·s)
ST2-127	87	9	4	99	2.48
ST2-126A	87	4	9	94	0.56
ST2-126B	87	0	13	91	0.72

laboratory lighting. Next, filtration of the functionalized copolymer was performed followed by its precipitation into approximately 300 mL of 4:1 methanol:water solution. The precipitate was stored in a 60 mL glass bottle that was wrapped with aluminum foil to avoid any exposure from ambient light and dried under vacuum at 65 °C for 24 h. The isolated yield of the functionalized copolymer was 90%. The reaction is depicted in Scheme 3. Three copolymers with different levels of cinnamate functionalization were synthesized for this study, and the compositions are provided in Table 1.

Differential scanning calorimetry (DSC) analysis of the functionalized copolymers was performed on a Perkin-Elmer Pyris 1 DSC at a heating rate of 10 °C/min under a nitrogen purge. The glass transition temperature (T_g) was determined from the second heat scan at the midpoint of the glass transition endotherm. The glass transition temperatures of the three functionalized copolymers are also listed in Table 1. UV−vis spectroscopy was performed on a Analytical Instrument Systems Inc. spectrometer that was equipped with fiber-optic light guides, a DT1000CE light source, and an Ocean Optics USB2000 UV−vis detector.

2.4. In Situ UV Irradiation during Electrospinning. The three functionalized copolymers were dissolved separately in DMF at a concentration of 20 wt %. Prior to electrospinning, the viscosities of these solutions were measured with a AR-1000 rheometer, TA Instruments Inc. The measurement was performed in the continuous ramp mode at room temperature (25 °C) using cone and plate geometry. The sample was placed between the fixed Peltier plate and a rotating cone (diameter: 4 cm; vertex angle: 2°) attached to the driving motor spindle. The changes in viscosity and shear stress with change in shear rate were measured. A computer interfaced to the equipment recorded the resulting shear stress vs shear rate data. For the three solutions investigated for the present study, the shear stress vs shear rate behavior was linear, indicating Newtonian behavior. The slope of the linear shear stress−shear rate relationships (valid in the range of 1−1000 s^{-1} for ST2-126A and B and 0−300 s^{-1} for ST2-127) gave the Newtonian or zero shear rate viscosities, η_0. These values are reported in Table 1. The viscosity of the polymer solutions is an important parameter that influences the final diameter of the electrospun fibers.[29,41,42] It is important to note, however, that the extensional viscosity of the jet while in flight to the target is undoubtedly very influential in governing the stretching induced in the jet. However, to the authors' knowledge, a thorough study of the effect of extensional viscosity on fiber formation in electrospinning has not been reported to date.

The schematic of the electrospinning apparatus with the UV source (F300S Fusion UV Systems, Inc., type "H" bulb') utilized for irradiation is shown in Figure 1. Electrospinning was performed in a vertical configuration where the fibers were electrostatically conveyed in the upward direction to the grounded target. This was done to minimize the heating effects that could arise from exposure to the highly intense UV beam. The apparatus was kept in a fume hood where an airflow was maintained from the bottom to top. The syringe containing the functionalized polymer solution was connected to a Teflon needle (0.7 mm i.d.). The free end of the Teflon needle was placed at the entrance of a 15 cm long quartz tube (15 cm i.d.). A grounded steel wire mesh that served as the target was placed 5 cm away from the other end of the quartz tube, and the total distance between the Teflon needle tip and target was 20 cm. A platinum electrode dipped in the polymer solution was connected to a high-voltage dc supply with positive polarity. A syringe pump connected to the syringe controlled the flow rate emanating out of the Teflon needle tip.

For each of the three solutions, electrospinning was performed at 15 kV, 3 mL/h, 20 cm at a concentration of 20 wt % in DMF. At the tip of the needle, the solution was observed to elongate into a conical shape, also referred to as the Taylor cone.[25] A jet was observed to emanate from the apex of the

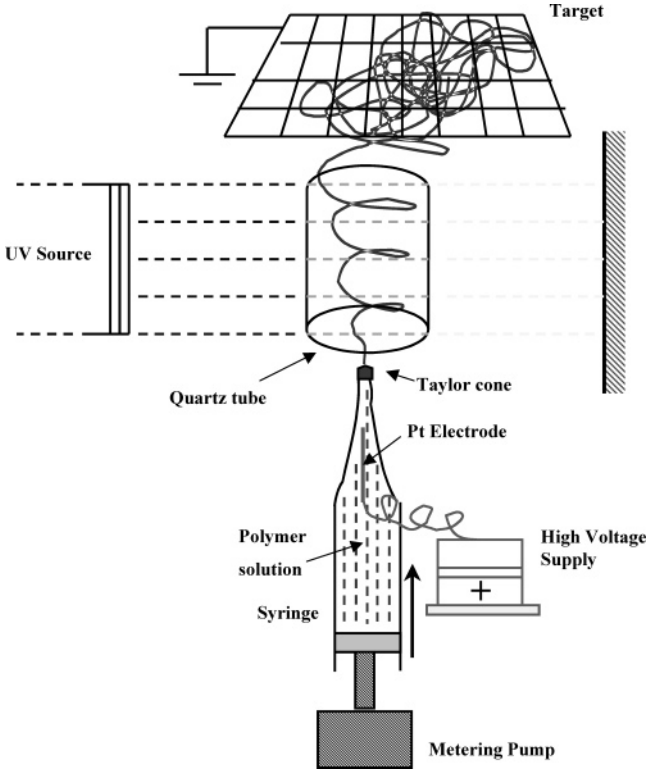

Figure 1. Schematic of the apparatus depicting the UV irradiation of eletrospun fibers.

Taylor cone that traveled through the quartz tube to the grounded target. During its travel through the quartz tube, the jet was exposed to the intense UV beam (UVB intensity of 0.135 W/cm^2) to allow for irradiation of the cinnamate groups. The quartz tube concentrates/partially focuses the UV beam on the spiraling and looping jet. Samples collected for 10 min with and without UV irradiation were dried in a vacuum at 40 °C for 8 h. A Leo 1550 field emission scanning electron microscope (FESEM) was utilized to visualize the morphology of the electrospun mat. A Cressington 208HR sputter-coater was utilized to sputter-coat the electrospun fiber samples with a 5 nm Pt/Au layer to minimize the electron charging effects. In addition, absorbance of the electrospun mats with and without UV irradiation was measured (in transmission mode) in the infrared region (4000−400 cm^{-1}) on a Nicolet 510 FTIR spectrometer. Gel fraction analysis of electrospun mats (with and without UV irradiation) was also conducted via a Soxhlet extraction process in refluxing THF for 4 h.

3. Results and Discussion

3.1. Synthesis and Modification of Poly(MMA-*co*-HEA). The precursor poly(MMA-*co*-HEA) copolymer was synthesized via an AIBN-initiated conventional free radical solution polymerization in ethyl acetate. The resulting copolymer exhibited an absolute weight-average molecular weight of 333 000 g/mol with a polydispersity of 1.96. The composition of the copolymer was examined using ^{1}H NMR spectroscopy. The results corresponded well with the feed ratios of 87 mol % MMA and 13 mol % HEA.

Modification of poly(MMA-*co*-HEA) with cinnamoyl chloride was conducted via an esterification reaction between the hydroxyl group of the HEA and cinnamoyl chloride (Scheme 3). Adjustment of the molar ratio of cinnamoyl chloride to the hydroxyl functionality was utilized to control the level of functionalization. Three functionalized MMA-*co*-HEA copolymers were synthesized with cinnamate concentrations of 4.0, 9.0, and 13 mol % (Table 1), utilizing the same precursor unfunctionalized copolymer mentioned previously. ^{1}H NMR spectroscopic analysis of the cinnamate functionalized poly(MMA-*co*-HEA) confirmed functionalization of the copolymers at three different levels of the cinnamate functionality. The resonances associated with the cinnamate group were apparent at 7.73, 7.52, 7.38, and 6.49 ppm. A reduction in the peak area of the methylene adjacent to the hydroxyl at 3.75 ppm was observed in addition to the corresponding appearance of the methylene resonance adjacent to an ester linkage at approximately 4.42 ppm. A typical UV absorbance spectrum of a cinnamate functionalized poly(MMA-*co*-HEA) is shown in Figure 2. An intense absorbance at 278 nm is characteristic of the vinylene C=C absorbance of the cinnamate group.[13,43,44] The UV absorbance of the precursor poly(MMA-*co*-HEA) is also shown in Figure 2 for comparison. As expected, the unfunctionalized copolymer does not show any distinct absorbance in the UVB region.

3.2. In Situ UV Irradiation during Electrospinning. As mentioned previously, a stable jet was observed to emanate from the apex of the Taylor cone at an electric field strength of 0.75 kV/cm that travels upward against gravity to the target maintained at ground potential. During its flight to the target, the jet was exposed to the intense unpolarized UV radiation that emanated as a parallel beam from the UV source. The dimensions of the beam emitted from the UV source were ca. 10 cm × 15 cm. The UVB intensity measured

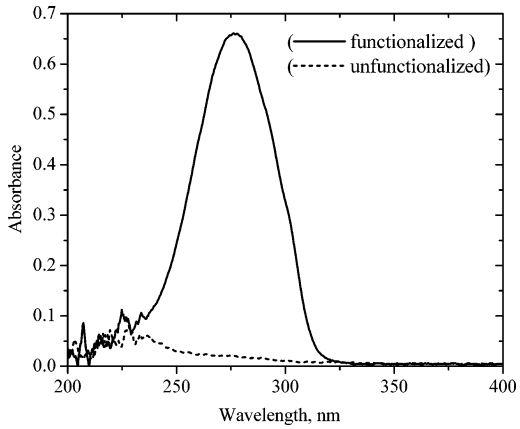

Figure 2. UV absorbance spectra of cinnamate functionalized (4 mol %) poly(MMA-*co*-HEA) compared to an unfunctionalized poly(MMA-*co*-HEA).

at the geometric midpoint of the quartz tube was 13.5 mW/cm^2. In an earlier study, Reneker et al. reported the measured jet velocity to be ca. 0.5 m/s.[27] On the basis of this value, it is estimated that the jet requires ca. 0.2 s to travel through the quartz tube. Hence, the UV beam should have sufficient intensity to allow adequate irradiation of the cinnamate group in 0.2 s or less. It was found, as will be discussed later, that at an estimated energy exposure of 2.7 mJ/cm^2 the cinnamate was able to undergo photodimerization, thereby leading to the formation of intermolecular cross-links within a given fiber. The aspect ratio of the electrospun jet increases as it undergoes the series of bending electrical instabilities,[27] leading to the exposure of a higher surface area to UV irradiation. Because of induced plastic stretching, the polymeric chains in the charged jet are believed to be in a partially extended state. Therefore, the probability of forming intermolecular cross-links is expected to be more favorable than the formation of intramolecular cross-links, although the latter cannot be discounted. A low vapor pressure solvent like DMF (bp 165 °C) does not rapidly evaporate from the jet. As a result, the polymer chains in the jet have sufficient mobility to intermingle and undergo intermolecular cross-linking. In a study involving investigations on formation of inter- and intramolecular cross-links in polymers, Coqueret et al.[45] stated that "if polymer chains intermingle freely, the likelihood of two adjacent reactant groups belonging to the same chain is small, thereby leading to the formation of mostly intermolecular links." In addition, intermolecular cross-links lead to an increase in the molecular weight of the polymer and eventually produce an insoluble gel, whereas intramolecular cross-links have no such effect. It is noted that the photodimerization of the cinnamate leads to cross-linking of the chains within a single electrospun fiber and not between the fibers. This was verified by easily pulling out the individual fibers from the irradiated mat by utilizing a pair of tweezers, thereby confirming that the fibers were not attached in the irradiated mat.

The SEM micrographs corresponding to fibrous mats (electrospun with and without UV irradiation) for the three terpolymers are shown in Figure 3. As expected, distinct morphological changes were not observed in the electrospun mats after irradiation. Uniform fibers of the functionalized copolymer containing the least amount of cinnamate (4 mol %) had a relatively larger diameter, ca. 2−4 μm, in comparison to the fibers of the other two

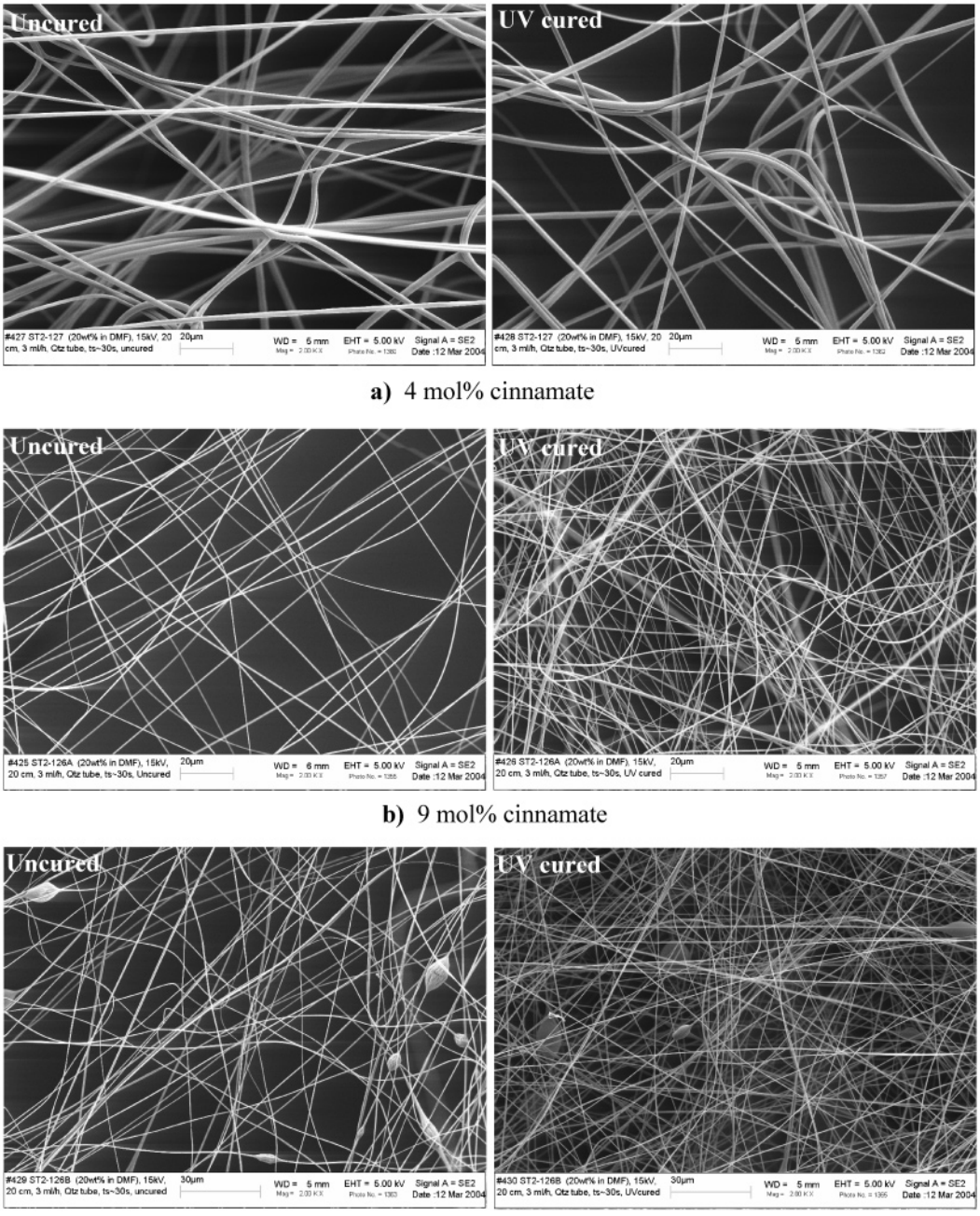

Figure 3. SEM micrographs of uncured and UV cured electrospun mats corresponding to (a) 4, (b) 9, and (c) 13 mol % cinnamate. Note that all the micrographs are at same magnification.

functionalized copolymers that both possessed a diameter of ca. 200−600 nm. This is due to the fact that the zero shear rate viscosity of the solution of functionalized copolymer with 4 mol % cinnamate was larger (2.48 Pa·s) than that of the other two solutions (0.56 and 0.72 Pa·s respectively for solutions of 9 and 13 mol % cinnamate-containing copolymers). Some "beaded" fibers were also observed to form in the case of the functionalized copolymer with the highest amount of cinnamate (13 mol %) (recall Figure 3). As reported earlier, the formation of beaded and uniform fibers was related to the polymer solution concentration and more specifically, viscosity.[29]

3.3. Photochemistry in the Electrospun Jet. As mentioned earlier, when cinnamates are exposed to UV, the cinnamate functional group undergoes either photoisomerization or photodimerization (Scheme 1). The intramolecular process of photoisomerization is generally favored in dilute solutions,[46] at least in the early stages of irradiation.[15−17] The photodimerization of cinnamates arises essentially from head-to-head and head-to-tail [$2\pi + 2\pi$] cycloaddition between the double bonds with favorable relative geometry (Scheme 2). Because of a brief lifetime of the excited states of benzene derivatives, the two chromophores must be very close to each other to facilitate the dimerization reaction.

The FTIR spectra of poly(MMA-*co*-HEA) cinnamate electrospun fibers (electrospun with and without UV irradiation) are shown in Figure 4. All observed vibrational bands were assigned in accordance with the results reported previously[18,47−52] (Table 2). In particular, the band at 1637 cm^{-1} corresponds to the vinylene C=C stretching vibration of the cinnamate group, while the bands at 1388 and 984 cm^{-1} correspond to the

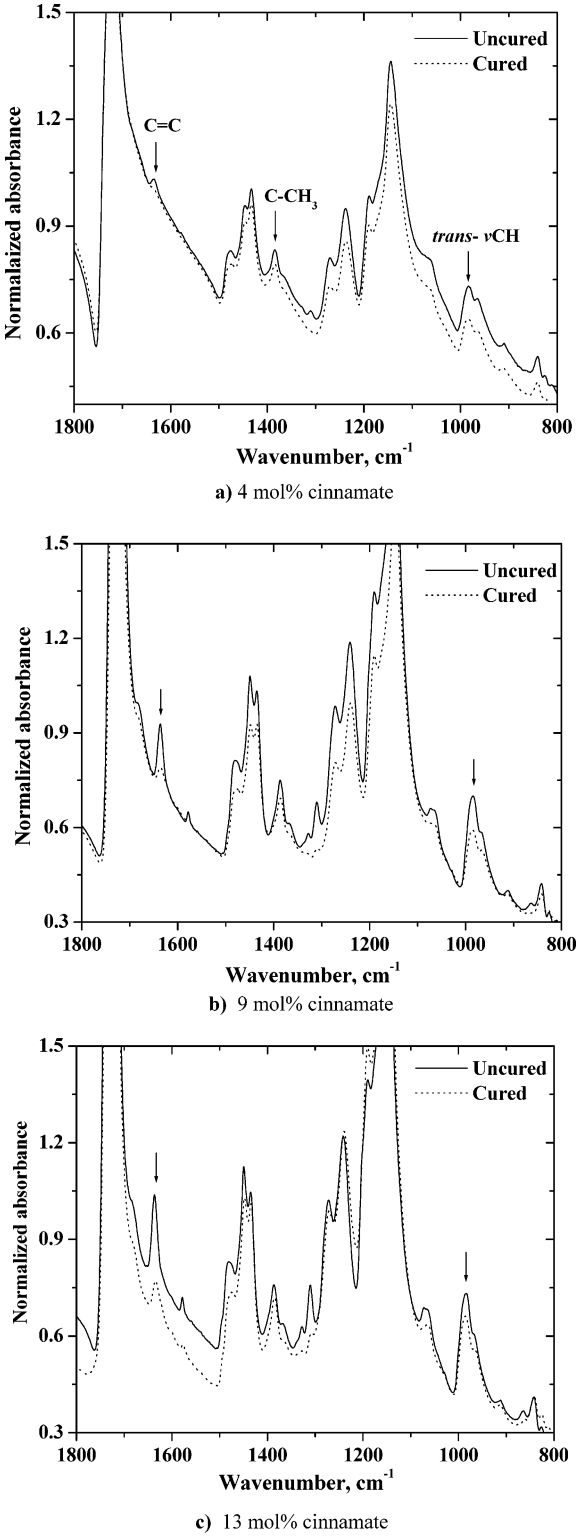

Figure 4. Absorbance FTIIR spectra of the uncured and UV cured electrospun mats containing (a) 4, (b) 9, and (c) 13 mol % cinnamate.

$C-CH_3$ bending vibration in MMA and the *trans*-vinylene C−H deformation of this same functional group, respectively. A flat baseline was not observed for the spectra reported here. This is due to the fact that the electrospun mats did not have a uniform cross-sectional composition (due to its porous nature). As the cross-sectional diameter of the detector IR beam was much larger (ca. 100 μm) than the diameter of the fibers (200 nm−4 μm), it is plausible that certain sections of the beam did not come in contact with solid fibers in the porous electrospun mat. As a result, a nonuniform signal was detected that lead to the nonflat baseline. However, when films cast from the same solutions were analyzed, FTIR peaks were observed to originate from the same minimum values of intensity leading to flat baselines. To compensate for thickness variations in the electrospun samples, the peak intensity at 1388 cm^{-1} corresponding to the bending vibration of the aliphatic $C-CH_3$ in MMA was used as a reference. This band was selected because the aliphatic $C-CH_3$ is not involved in the photochemical reactions.

Table 2. Characteristic IR Bands of Poly(MMA-*co*-HEA) Cinnamate

wavenumber (cm^{-1})	assignment description in IR
1637	C=C stretching vibration of cinnamate
1388	$C-CH_3$ bending vibration of atactic PMMA
984	*trans*-vinylene CH deformation vibration of cinnamate
887	*cis*-vinylene CH deformation vibration of cinnamate

As observed in Figure 4, in all three functionalized copolymers, the intensities of the bands at 1637 and 984 cm^{-1} (due to the vinylene C=C stretching and *trans*-vinylene C−H deformation vibration of the cinnamate groups, respectively) decreased with UV irradiation. The intensity drop in the vinylene C=C stretching band results from the conversion of the cinnamate groups due to the photodimerization (Scheme 2), while the intensity drop in the *trans*-vinylene C−H deformation vibrational band is distinctly attributed to the consumption of the *trans*-vinylene linkage in the cinnamate group due to trans−cis photoisomerization (recall Scheme 1) and photodimerization. To evaluate the relative reactivity of these two photoreactions, the following relationships are defined:

$$F_{1637} = 1 - \frac{(I_{1637}/I_{1388})_i}{(I_{1637}/I_{1388})_o} \quad (1)$$

$$F_{984} = 1 - \frac{(I_{984}/I_{1388})_i}{(I_{984}/I_{1388})_o} \quad (2)$$

where $(I_{1637}/I_{1388})_i$ corresponds to the relative intensity of the vinylene C=C bonds *after* irradiation and $(I_{1637}/I_{1388})_o$ is the relative intensity of the C=C bonds *before* irradiation. Likewise, in eq 2, F_{984} quantifies the consumption of *trans*-cinnamate functional groups during trans−cis photoisomerization. For the electrospun mats corresponding to the three functionalized copolymers, the values of F_{1637} obtained were 0.008, 0.117, and 0.178 respectively for 4, 9, and 13 mol % of cinnamate incorporated in the copolymer. As expected, the F_{1637} values increase systematically with increasing mol % of the photocurable cinnamate functional group (Figure 5). However, at 4 mol % functionalization, only a *very* small fraction (0.8%) of the cinnamate groups undergo photodimerization. Mathematically, this translates to about 0.54 cross-links per chain in the 4 mol % (calculation based on the number-average molecular weight of ca. 170 000 g/mol) cinnamate functionalized copolymer, indicating the statistical impossibility for the copolymer to form a well developed cross-linked network. At 9 and 13 mol % functionalization, the calculated numbers of cross-links per chain are 17 and 39, respectively, which

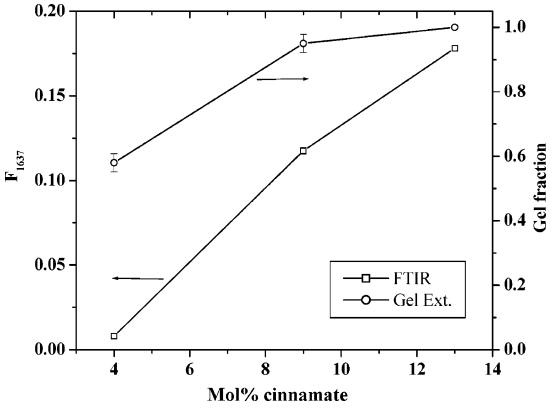

Figure 5. Comparison of the extent of cross-linking as measured by absorbance FTIR and solvent gel extraction.

in turn is equivalent to a molecular weight of 10 000 and 4400 g/mol between cross-links, respectively. The values of F_{984} for the three systems were 0.052, 0.030, and 0.057 respectively for 4, 9, and 13 mol % of cinnamate incorporated in the copolymer. The small positive values of F_{984} indicated that a low level of photoisomerization also took place during the UV irradiation. It is important to note that at 4 mol % functionalization a higher value of F_{984} than F_{1637} indicates the dominance of photoisomerization over photodimerization. This is attributed to a lesser concentration of cinnamate functional groups. Upon UV irradiation these functional groups undergo photoisomerization instead of photodimerization due to a lack of other cinnamate groups in the immediate vicinity. As the concentration of these functional groups increases, the probability of finding any two spatially close cinnamate groups increases, thereby leading to photodimerization—an observation corroborated by the larger values of F_{1637} than F_{984} at 9 and 13 mol % functionalization, respectively.

The irradiated and nonirradiated electrospun mats were also investigated in terms of gel fractions (Soxhlet extraction process in refluxing THF for 4 h). The nonirradiated electrospun mats did not exhibit any gel formation (the measured gel fraction was zero for the each of the three systems investigated). For the irradiated electrospun mats, the gel fraction values are plotted in Figure 5 (secondary axis). It can be seen that a gel fraction of 58% was attained at 4 mol % cinnamate content. At 9 mol %, nearly 95% gel formation occurred whereas at 13 mol % a 100% gel was observed to form. Recalling the earlier discussion, these results clearly indicated the formation of intermolecular cross-linking due to the photodimerization of the cinnamate functional group. At 9 and 13 mol % of cinnamate content, the irradiated functionalized copolymer formed high levels of gel fraction (95% and 100%, respectively), thereby indicating that photodimerization of the cinnamate functional group was the primary photoprocess during UV irradiation.

4. Conclusions

A *novel* approach to in situ cross-link polymeric fibers that were produced during electrospinning was demonstrated. The *modified* electrospinning apparatus that facilitates in situ UV irradiation of electrospun fibers was described. Copolymers of MMA and HEA were synthesized and subsequently functionalized with cinnamoyl chloride. Three functionalized copolymers with different mol % of the cinnamate group (4, 9, and 13 mol %) were utilized in this study. Electrospun fibers of cinnamate functionalized poly(MMA-*co*-HEA) were successfully cross-linked with UV radiation *while in flight* to the collector target. Subsequent FTIR measurements on UV irradiated and nonirradiated electrospun fibers indicated the $[2\pi + 2\pi]$ cycloaddition of the vinylene C=C in addition to the trans−cis photoisomerization of the cinnamate species. At 4 mol % functionalization, photoisomerization was the dominant process due to a very low concentration of cinnamate. Further, the irradiated electrospun mats were observed to form an insoluble gel fraction, indicating the formation of intermolecular cross-links. It was noted that the photodimerization of cinnamate lead to cross-linking between the chains within a single electrospun fiber and not between the fibers.

Acknowledgment. This material is based upon work supported by, or in part by, the U.S. Army Research Laboratory and the U.S. Army Research Office under Grant DAAD19-02-1-0275 Macromolecular Architecture for Performance (MAP) MURI. The authors thank Prof. Chip Frazier, Wood Science Department, Virginia Tech, for allowing the use of AR-1000 rheometer for viscosity measurements.

References and Notes

(1) Visconte, L. L. Y.; Andrade, C. T.; Azuma, C. *J. Appl. Polym. Sci.* **1998**, *69*, 907−910.
(2) Minsk, L. M.; Smith, J. G.; Deusen, W. P. V.; Wright, J. F. *J. Appl. Polym. Sci.* **1959**, *2*, 302−307.
(3) Kvasnikov, E. D.; Kozenkov, V. M.; Barachevsky, V. A. *Zh. Nauchn. Prikl. Fotogr. Kinematogr.* **1979**, *24*, 222.
(4) Barachevsky, V. A. *SPIE* **1991**, *1559*, 184.
(5) Gibbons, W. M.; Shannon, P. J.; Sun, S. T.; Swetlin, B. J. *Nature (London)* **1991**, *351*, 49.
(6) Gibbons, W. M.; Shannon, P. J.; Sun, S. T. *Mol. Cryst. Liq. Cryst.* **1994**, *251*, 191.
(7) Shannon, P. J.; Gibbons, W. M.; Sun, S. T. *Nature (London)* **1994**, *368*, 532.
(8) Iimura, Y.; Kusano, J.; Kobayaashi, S.; Aoyagi, T. T. S. *Jpn. J. Appl. Phys., Part 2* **1993**, *32*, L93.
(9) Kawanishi, Y.; Tamaki, T.; Sakuragi, M.; Seki, T.; Suzuki, Y.; Ichimura, K. *Langmuir* **1992**, *8*, 2601.
(10) Kawanishi, Y.; Tamaki, T.; Sakuragi, M.; Seki, T.; Ichimura, K. *Mol. Cryst. Liq. Cryst.* **1992**, *218*, 153.
(11) Ichimura, K.; Hayashi, Y.; Akiyama, H.; Ikeda, T.; Ishizuki, N. *Appl. Phys. Lett.* **1993**, *63*, 449.
(12) Robertson, E.; Deusen, W.; Minsk, L. *J. Appl. Polym. Sci.* **1959**, *2*, 308−311.
(13) Zheng, Y. J.; Andreopoulos, F. M.; Micic, M.; Huo, Q.; Pham, S. M.; Leblanc, R. M. *Adv. Funct. Mater.* **2001**, *11*, 37−40.
(14) Kimura, T.; Kim, J.-Y.; Fukuda, T.; Matsuda, H. *Macromol. Chem. Phys.* **2002**, *203*, 2344−2350.
(15) Kawatsuki, N.; Matsuyoshi, K.; Hayashi, M.; Takatsuka, H.; Yamamoto, T.; Sangen, O. *Chem. Mater.* **2000**, *12*, 1549.
(16) Rennert, J. J. *Photogr. Sci. Eng.* **1971**, *15*, 60.
(17) Graley, M.; Reiser, A.; Roberts, A. J.; Phillips, D. *Macromolecules* **1981**, *14*, 1752.
(18) Chae, B.; Lee, S. W.; Ree, M.; Jung, Y. M.; Kim, S. B. *Langmuir* **2003**, *19*, 687−695.
(19) Ichimura, K.; Akita, Y.; Akiyama, H.; Kudo, K.; Hayashi, Y. *Macromolecules* **1997**, *30*, 903−911.
(20) Doshi, J.; Reneker, D. H. *J. Electrostat.* **1995**, *35*, 151−160.
(21) Fong, H.; Chun, I.; Reneker, D. H. *Polymer* **1999**, *40*, 4585−4592.
(22) Kim, J.-S.; Reneker, D. H. *Polym. Eng. Sci.* **1999**, *39*, 849−854.
(23) Deitzel, J. M.; Kleinmeyer, J. D.; Hirvonen, J. K.; Beck, T. N. C. *Polymer* **2001**, *42*, 8163−8170.
(24) Srinivasan, G.; Reneker, D. H. *Polym. Int.* **1995**, *36*, 195−201.
(25) Taylor, G. I. *Proc. R. Soc. London* **1964**, *280*, 383−397.
(26) Yarin, A. L.; Koombhongse, S.; Reneker, D. H. *J. Appl. Phys.* **2001**, *90*, 4836−4846.

(27) Reneker, D. H.; Yarin, A. L.; Fong, H.; Koombhongse, S. *J. Appl. Phys.* **2000**, *87*, 4531−4547.
(28) Hohman, M. M.; Shin, M.; Rutledge, G.; Brenner, M. P. *Phys. Fluids* **2001**, *13*, 2201−2220.
(29) McKee, M. G.; Wilkes, G. L.; Colby, R. H.; Long, T. E. *Macromolecules* **2004**, *37*, 1760−1767.
(30) Wang, X.; Lee, S.-H.; Drew, C.; Senecal, K. J.; Kumar, J.; Samuelson, L. A. *Polym. Mater.: Sci. Eng.* **2001**, *85*, 617−618.
(31) Zhang, Y.; Dong, H.; Norris, I. D.; MacDiarmid, A. G.; Jones, W. E. *Polym. Mater.* **2001**, *85*, 622−623.
(32) Fong, H.; Liu, W.; Wang, C.-S.; Vaia, R. A. *Polymer* **2002**, *43*, 775−780.
(33) Deitzel, J. M.; Kosik, W.; McKnight, S. H.; Tan, N. C. B.; DeSimone, J. M.; Crette, S. *Polymer* **2002**, *43*, 1025−1029.
(34) Boland, E. D.; Wnek, G. E.; Simpson, D. G.; Pawlowski, K. J.; Bowlin, G. L. *J. Macromol. Sci., Pure Appl. Chem.* **2001**, *A38*, 1231−1243.
(35) Matthews, J. A.; Wnek, G. E.; Simpson, D. G.; Bowlin, G. L. *Biomacromolecules* **2001**, *3*, 232−238.
(36) Kenaway, E.-R.; Bowlin, G. L.; Mansfield, K.; Layman, J.; Simpson, D. G.; Sanders, E. H.; Wnek, G. E. *J. Controlled Release* **2002**, *81*.
(37) Gibson, P.; Schreuder-Gibson, H.; Pentheny, C. *J. Coated Fabr.* **1998**, *28*, 63−72.
(38) Pinto, N. J.; Carrion, P.; Quinones, J. X. *Mater. Sci. Eng.* **2004**, *A366*, 1−5.
(39) Son, K. S.; Youk, H. J.; Park, W. H. *Biomacromolecules* **2004**, *5*, 197−201.
(40) Zeng, J.; Hou, H.; Wendorff, J. H.; Greiner, A. *Polym. Prepr. (Am. Chem. Soc., Div. Polym. Chem.)* **2003**, *44*, 174−175.
(41) Yarin, A. L.; Koombhongse, S.; Reneker, D. H. *J. Appl. Phys.* **2001**, *90*, 4836−4846.
(42) Buer, A.; Ugbolue, S. C.; Warner, S. B. *Textile Res. J.* **2001**, *71*, 323−328.
(43) Lazarev, V. V.; Barberi, R.; Iovane, M.; Papalino, L.; Blinov, L. M. *Liq. Cryst.* **2002**, *29*, 273−279.
(44) Nakayama, Y.; Matsuda, T. *J. Polym. Sci., Polym. Chem.* **1992**, *30*, 2451−2457.
(45) Reiser, A.; Egerton, P. L. *Macromolecules* **1979**, *12*, 670−673.
(46) Coqueret, X.; El Achari, A.; Hajaiej, A.; Lablache-Combier, A.; Loucheux, C.; Randrianarisoa, L. *Makromol. Chem.* **1991**, *192*, 1517.
(47) Schneider, B.; Stokr, J.; Schmidt, P.; Mihailov, M.; Dirlikov, S.; Peeva, N. *Polymer* **1979**, *20*, 705−712.
(48) Dybal, J.; Krimm, S. *Macromolecules* **1990**, *23*, 1301−1308.
(49) Perny, S.; Le Barny, P.; Delaire, J.; Buffeteau, T.; Sourisseau, C. *Liq. Cryst.* **2000**, *27*, 341−348.
(50) Perny, S.; Le Barny, P.; Delaire, J.; Buffeteau, T.; Sourisseau, C.; Dozov, I.; Forget, S.; Martinot-Lagarde, P. *Liq. Cryst.* **2000**, *27*, 329−340.
(51) Perny, S.; Le Barny, P.; Delaire, J.; Dozov, I.; Forget, S.; Auroy, P. *Liq. Cryst.* **2000**, *27*, 349−358.
(52) Oriol, L.; Pinol, M.; Serrano, J. L.; Tejedor, R. M. *J. Photochem. Photobiol. A* **2003**, *155*, 37−45.

MA048844G